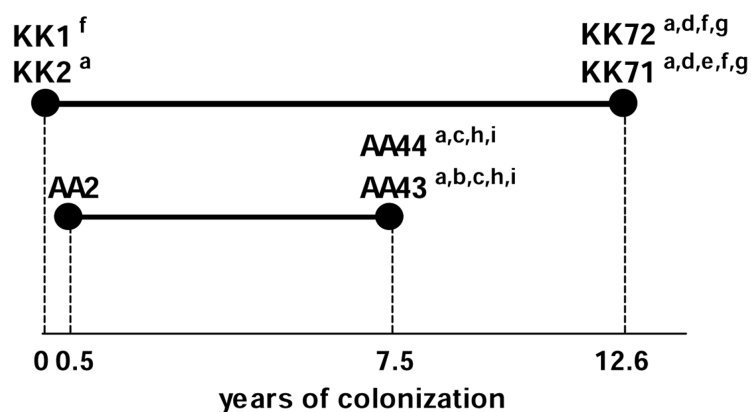


**Tracking the immunopathological response to *Pseudomonas aeruginosa* during respiratory infections**

Cristina Cigana, Nicola Ivan Lorè, Camilla Riva, Ida De Fino, Lorenza Spagnuolo, Barbara Sipione, Giacomo Rossi, Alessandro Nonis, Giulio Cabrini, Alessandra Bragonzi

**Supplementary Information**

## SUPPLEMENTARY FIGURES AND LEGENDS



**Fig. S1. Genotypic and phenotypic characteristic of *P. aeruginosa* sequential isolates from CF patients.** Sequential *P. aeruginosa* isolates were recovered at the onset of chronic colonization (AA2, KK1, KK2) or several years after acquisition and before patient's death (AA43, AA44, KK71, KK72). Clonality of strains was assessed by Pulsed Field Gel Electrophoresis and was previously reported <sup>1</sup>. Multiple phenotypic traits changed during genetic adaptation to the CF lung <sup>2</sup> and included: (a) motility defect, (b) mucoid phenotype, (c) protease reduction, (d) siderophore reduction, (e) hemolysis reduction, (f) *LasR* mutant phenotype, (g) growth rate reduction. In addition, lipopolysaccharide (LPS) lipid A (h) and peptidoglycan (PGN) muropeptides (i) were analyzed exclusively in the AA isolates showing specific structural modifications temporally associated with CF lung infection as previously described <sup>3</sup>.

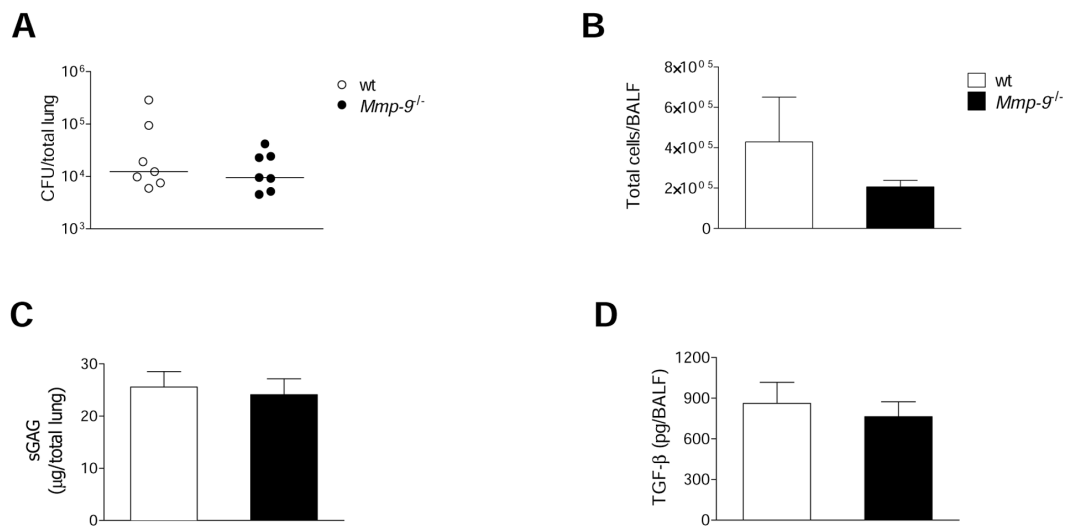


**Fig. S2. Bacterial load, leukocytes recruitment and tissue damage in lungs of *Mmp-9*<sup>-/-</sup> and congenic wt mice after *P. aeruginosa* long-term chronic infection.** B6.FVB(Cg)-Mmp9tm1Tvu/J and congenic mice were infected with 2x10<sup>6</sup> CFU/lung of AA43 strain embedded in agar beads. **A)** CFU in total lung, **B)** total cells recruitment in BALF, **C)** sGAG in lung homogenate by a colorimetric assay and **D)** TGF-β<sub>1</sub> by Bioplex were evaluated after 28 days of chronic lung infection with the *P. aeruginosa* CF-adapted isolate AA43. Dots represent CFUs in individual mice and horizontal lines represent median values. Total leukocytes, sGAG and TGF-β<sub>1</sub> values are represented as mean ± SEM. The data derive from one experiment (n=6-7).

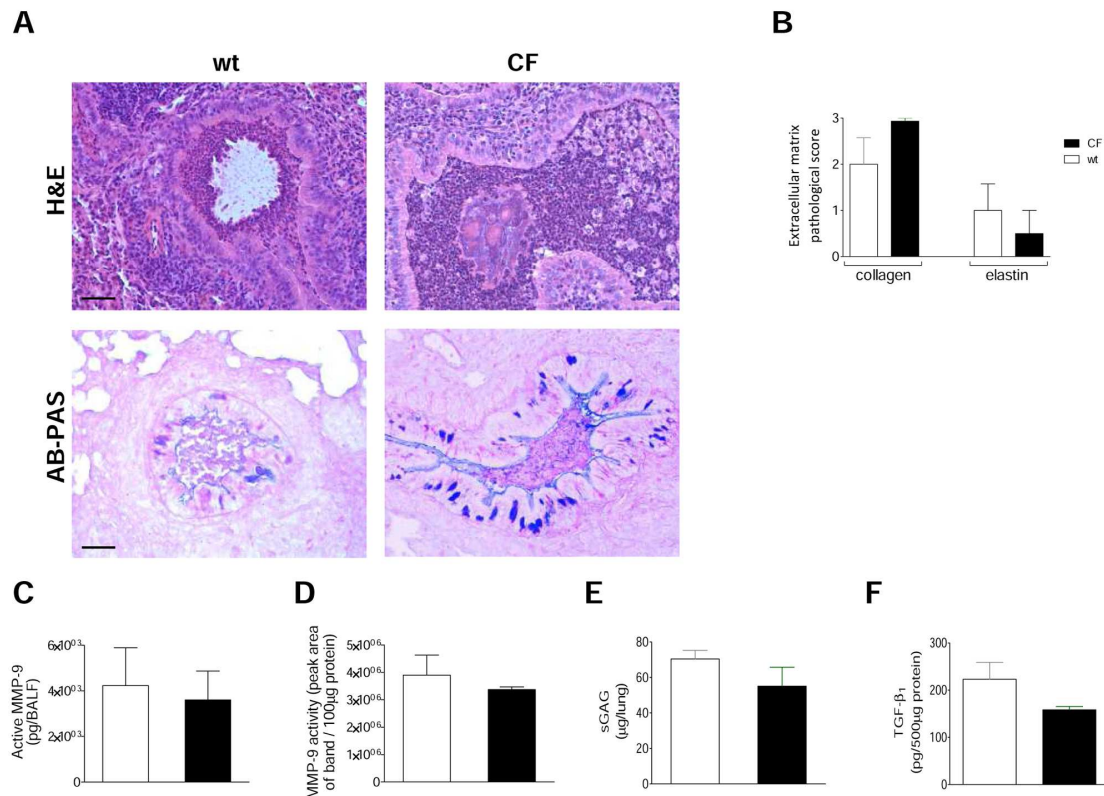


**Fig S3. Tissue damage after *P. aeruginosa* lung chronic infection in CF and wt mice.** Gut-corrected CFTR-deficient C57Bl/6  $Cftr^{tm1UNC}TgN(FABPCFTR)\#Jaw$  (CF) and congenic wt mice were infected with  $2 \times 10^6$  CFU/lung of *P. aeruginosa* AA43 isolate embedded in agar beads for 28 days. Sections of murine lungs were stained with H&E and AB/PAS (A) for mucopolysaccharides, according to the standard procedure. Scale bars: 50  $\mu$ m. Scorings of collagen deposition and elastin degradation (B) were performed on slices stained with MTS and VEG, respectively. Levels of MMP-9 protein (C) in BALF by ELISA, MMP-9 activity (D) in lung homogenate by zymography, sGAG (E) in lung homogenate by a dye-binding colorimetric assay and TGF- $\beta_1$  (F) in lung homogenate by Bioplex were measured after 28 days of chronic lung infection with the *P. aeruginosa* CF-adapted isolate AA43. Values represent the mean  $\pm$  SEM. The data are pooled from two independent experiments (n=3-11).

1 **Table S1**  
2

Gene name	Gene symbol	Alternative common names	Macroarray results (relative to AA2)		Validation results	
			AA43 vs AA2	AA44 vs AA2	Folds of induction [Mean $\pm$ SEM (N)]	
					AA43 vs AA2	AA44 vs AA2
Gro-b (Growth-regulated protein beta)	CXCL2	MIP-2a	down	down	0,53 $\pm$ 0.071 (N=5)	0.63 $\pm$ 0.085 (N=5)
Gro-g	CXCL3	MIP-2b	down	down	1.05 $\pm$ 0.213 (N=3)	0.95 $\pm$ 0.26 (N=3)
IL-8 (interleukin-8)	CXCL8		down	down	0.59 $\pm$ 0.041 (N=4)	0.54 $\pm$ 0.057 (N=4)
IP-10 (Interferon gamma-induced protein 10)	CXCL10	small-inducible cytokine B10	down	down	0.56 $\pm$ 0.111 (N=6)	0.67 $\pm$ 0.085 (N=6)
Angie	CXCL13	BLC (B lymphocyte chemoattractant)	up	up	nd	nd
C-C receptor 6	CCR6	cluster of differentiation (CD) 196	down	down	nd	nd
C-C receptor 7	CCR7	CD197	down	down	nd	nd
C-C receptor 9	CCR9	CDw199	down	down	nd	nd
CXC receptor 6	CXCR6	CD186	up	up	nd	nd

Intercellular adhesion molecule 1	ICAM-1	CD54	down	down	0.59 ± 0.117 (N=3)	0.51 ± 0.123 (N=3)
Vascular cell adhesion molecule 1	VCAM-1	CD 106	down	down	0.35 ± 0.072 (N=4)	0.61 ± 0.059 (N=4)
Adiponectin	ADIPOQ	GBP-28, apM1, Acrp30	down	down	nd	nd
Tumor Necrosis Factor alpha	TNF-a	cachexin	down	down	0.61 ± 0.047 (N=4)	0.58 ± 0.037 (N=4)
Toll-like receptor 2	TLR-2	CD282	down	down	0.96 ± 0.15 (N=3)	0.99 ± 0.057 (N=3)
Toll-like receptor 5	TLR-5		up	up	1.12 ± 0.12 (N=3)	1.24 ± 0.107 (N=3)
Human Defensin b1	HDB-1	DEFB1	up	up	nd	nd
Dual oxidase 2	FPR2	FPRL1	down	down	nd	nd
Statherin	STATH		down	down	nd	nd
Elastase 2	ELA2		down	down	0.89 ± 0.217 (N=3)	0.95 ± 0.34 (N=3)
Matrix metalloprotease 9	MMP-9	gelatinase B	up	up	0.97 ± 0.136 (N=4)	1.06 ± 0.101 (N=4)

3  
4

nd: not determined

## 5 SUPPLEMENTARY METHODS

6 **Infection of cell lines.** IB3-1 and C38 cells were infected with *P. aeruginosa* isolates  
7 at a multiplicity of infection (MOI) of 0.1 for 4 h for RNA extraction and at a MOI of  
8 1 for 2 h for analysis of IL-8 levels as previously described <sup>4</sup>. THP-1 cells were  
9 seeded and differentiated to macrophage-like cells as described previously <sup>5</sup>, then  
10 infected for 4 h with *P. aeruginosa* isolates at a MOI of 1. Growth media were  
11 collected at the end of incubation, centrifuged and stored at –80°C for analysis of  
12 MMP-9.

13

### 14 **Macroarray analysis and validation**

15 Total RNA was extracted from lysed cells with the Total RNA Isolation kit (Roche),  
16 converted to cDNA with High Capacity cDNA Archive Kit (Applied Biosystems) and  
17 random primers.

18 In this study, the expression of 92 target genes, that are crucial in the first line of  
19 response against pathogens and critical in chronic inflammatory diseases of the  
20 airways, were obtained using TaqMan Low Density Array (TLDA) platform (Applied  
21 Biosystems, Foster City, CA), as previously described (1). To validate the data,  
22 separate quantitative Real-Time Polymerase Chain Reaction (qRT-PCR) experiments  
23 were performed as previously described (1-2). IL-8 and MMP-9 protein releases were  
24 measured with ELISA assays, according to the manufacturer's protocols (R&D).

25

### 26 **Histological examination**

27 Murine and human lungs were removed, fixed in formalin, and embedded in paraffin.  
28 Consecutive sections from the middle of the five lung lobes were used for  
29 histological, immunohistochemical, and immunofluorescence examination in each

30 mouse. Indirect immunofluorescence was performed using a polyclonal rabbit anti-*P.*  
31 *aeruginosa* Ab (kindly provided by G.B. Pier, Harvard Medical School, Boston, MA).  
32 The secondary Ab was Texas Red-labeled goat anti-rabbit Ig G (Molecular Probes).  
33 The slides were examined using an Axioplan fluorescence microscope (Zeiss), and  
34 images were taken with a KS 300 imaging system (Kontron). Sections for histological  
35 analysis were stained by H&E, Alcian Blue-Periodic Acid Schiff (AB-PAS),  
36 Masson's trichrome (MTS) and Verhoeff's elastic (VEG) staining and were examined  
37 blindly and scored by a pathologist, as describe below.

38 Bronchial epithelial degeneration was performed on lung sections stained with  
39 Haematoxylin-Eosin as previously described <sup>6</sup>.

40 Histological score analysis of murine lungs was performed to grade the amount of  
41 innate immune cells infiltration and BALT activation. Histological examination  
42 primarily included the assessment of cellular infiltrates and aggregation by scoring the  
43 number of immune cells (mononuclear cells, such as macrophages, lymphocytes,  
44 plasma cells, and neutrophils) at a magnification of  $\times 400$ . The number of  
45 inflammatory cells was evaluated by using a visual analogue scale modified for  
46 murine pulmonary specimens, as described previously <sup>7</sup>, and results are reported as  
47 the mean for the entire specimen. When considerable heterogeneity of infiltration was  
48 evident in the same specimen, the mean for several areas was determined and the  
49 specimen was scored accordingly. Neutrophils and macrophages were classified as  
50 absent (score of 0) when there were no or fewer than 19 cells per high-power field  
51 (HPF) (at a magnification of  $\times 400$ ), mild (score of 1) for 20 to 49 cells per HPF,  
52 moderate (score of 2) for 50 to 99 cells per HPF, marked or severe (score of 3) for  
53 100 to 200 cells or more per HPF. Histological criteria for normal pulmonary  
54 characteristics included detection of no or only a few mononuclear cells per HPF and



55 no or only a few scattered neutrophils in bronchioli and alveoli without tissue changes  
56 (no interstitial thickening or aggregates of lymphocytic infiltrates, and airways free  
57 from exudate). The number of inflammatory cells and of lymphoid aggregates,  
58 assessed at  $\times 400$  and  $\times 100$  magnification respectively, was scored and customized as  
59 described by Martino et al <sup>8</sup>.

60 Histologic lesions of the respiratory bronchial epithelium were evaluated and scored  
61 for the presence or absence of ciliated columnar cells, goblet cells, edema, hyperplasia  
62 or metaplasia of epithelial cells, and lymphocytes infiltration (see also the scoring  
63 system to evaluate adaptive immunity), based on the previously described scoring  
64 system <sup>9-11</sup>: presence of ciliated columnar epithelium, normal goblet cells, and no  
65 lymphocyte infiltration in respiratory epithelium (score 1); presence of focal lesions,  
66 some degenerative or necrotic epithelial cells, small focal areas lacking cilia, no  
67 lymphocyte infiltration in respiratory epithelium (score 2); multifocal areas lacking  
68 cilia accompanied by edema, degenerative and hyperplastic changes in epithelial cells,  
69 locally disrupted epithelial layer, infiltration of lymphocytes (score 3); diffuse or  
70 severe lesions showing replacement of normal ciliated columnar epithelial lining by  
71 the squamous to cuboidal epithelium without cilia, disrupted epithelial layer in many  
72 places, depletion of goblet cells, and infiltration of lymphocytes into respiratory  
73 epithelium (score 4). The sums of scores of bronchial lesions for mouse in one group  
74 were summed, and was used for statistical comparison of the severity lesions between  
75 the groups. Finally, concerning histological scores indicating an adaptive immune  
76 response, the presence of lymphoid nodules consisting of 5 to 7 lymphocyte-like cells  
77 (germinal centers) within areas of secondary bronchi and blood vessels, the intensity  
78 of dispersed lymphocyte infiltration in the interalveolar septa and interparabronchial  
79 septum and around the secondary bronchi as well as around the blood vessels was

80 evaluated and recorded. The score was calculated as follow: no lymphocyte  
81 accumulation in interalveolar and interparabronchial septa, and very few germinal  
82 centers around secondary bronchi and blood vessels (score 0); accumulation of a few  
83 dispersed lymphocytes without the increase of the number of germinal centers (score  
84 1); moderate accumulation of lymphocytes in interalveolar and interparabronchial  
85 septa, increased size of germinal centers (group of 10–13 cells) around blood vessels  
86 (score 2); thickened interatrial septa in a large area of the lung, interparabronchial  
87 septa infiltrated with histiocytes and lymphocytes, and increased number of germinal  
88 centers (score 3). The sum of scores of the mice in one group was used for statistical  
89 comparison of the severity of bronchial lesions and mononuclear cells system  
90 activation between the groups.

91 For BALT activation, the score was assessed at  $\times 100$ , by calculating the total areas of  
92 BALT follicles evaluated inside each lung section, and subdividing the mean as  
93 follow: mean area of BALT follicle extension none (score 0); up to 0.008 square mm  
94 (score 1); up to 0.042 square mm (score 2); up to 0.4 square mm (score 3).

95 For evaluation the degree of fibrosis in lungs, Masson's trichrome-stained (MTS)  
96 sections were assessed as follow: the areas of lung fibrosis were represented as blue-  
97 stained areas, and the parenchyma as red-stained regions by MTS. The total area of  
98 the section was the sum of the area of all microscopic fields, including parenchyma  
99 and fibrosis. Elements of the pleura were excluded from the computations. Then the  
100 percentage of bluish-green stain, representing the area of fibrosis for each lung section  
101 specimen, was calculated using the Leica Qwin 500 Image Analyzer (Leica,  
102 Cambridge, England), to capture the widest area of tissue. Images of trichrome  
103 stained sections were captured using a  $\times 5$  HPFs and the area of the section was the  
104 sum of the area of all microscopic fields, including parenchyma and fibrosis. The

105 scoring system was characterized as follow: normal lung (score 0); lungs showing a  
106 minimum percentage of fibrosis (percentage area of fibrosis  $\geq 1.709$ ;  $\leq 6.899$ ; mean  
107 area 4,304) (score 1); moderate ( $\geq 6.899$ ;  $\leq 10.798$ ; mean percentage area 8.848)  
108 (score 2); severe (corresponding to an area  $\geq 10.798$ ; until 32.498 and over; mean  
109 percentage area 19,215) (score 3).

110 Verhoeff's elastic stains (VES) was used for assessing and quantifying the elastin  
111 architecture in lung interstitial and peribrochial areas. The degree of fragmentation  
112 and the amount of the elastic fibers were examined by the pathologist, blinded to the  
113 treatment group, who scored each slide using an arbitrary combined scoring system  
114 that counted the number of "islands of damage" within a lung cross-section from each  
115 mouse. An island of damage was defined as an isolated area of lung's interstitium or  
116 peribronchus, where two adjacent elastic fibers were fragmented with interposed  
117 excessive connective tissue matrix, evaluated randomly on the cross-section at x 400.  
118 Three evaluations were performed per lung. The method was extrapolated from  
119 McLoughlin *et al.*<sup>12</sup>.

120

121 **Evaluation of markers associated to tissue damage.** Murine active MMP-9 and  
122 sGAG were measured respectively by ELISA (R&D) and by sGAG assay (Kamiya  
123 Biomedical Company), according to the manufacturers' instructions. Collagen was  
124 quantified by Sircol Collagen Assay (Biocolor Life Science) according to  
125 manufacturer's instructions. Gelatinase zymography was performed to evaluate the  
126 activity of MMP-9 (gelatinase B) in murine BALF and lung homogenates<sup>13</sup>. Protein  
127 concentration was determined; 100  $\mu\text{g}$  of lung homogenates were analyzed.  
128 Supernatants (SN) from macrophages-like cells THP-1 were used as positive control.  
129 Samples and molecular weight (BlueStar Protein Marker; Life Science) were

130 electrophoresed on precast polyacrilamide gel with gelatine (10%). After  
131 electrophoresis the gels were incubated in Renaturing Solution (2,5% Triton X-100)  
132 for 30 min at room temperature. The gels were equilibrated in Developing Solution  
133 (50 mM Tris, 200mM NaCl, 5mM CaCl<sub>2</sub> and 0,02% Brij-35, pH 7.5) for other 30  
134 minutes and then incubated at 37°C in the same buffer for 24 hrs. They were stained  
135 for 40 minutes with Staining Solution (0,5 % Comassie Brilliant Blue in 45%  
136 methanol and 10% acetic acid) and then destained for 2 hrs with Destaining Solution  
137 (45% methanol and 10% acid acetic). Zones of murine and human MMP-9 proteolysis  
138 appeared as clear bands against a blue background at approximately 92 kDa and 85  
139 kDa respectively. Band intensities were measured by ImageJ. Data obtained were  
140 normalized to the value of the positive control.

141

#### 142 **Cytokines/chemokines quantification**

143 Bio-Plex<sup>®</sup> multiplex system was used for the quantification of cytokines/chemokines  
144 and growth factors, according to the manufacturer's instruction. In details, Multiplex  
145 immunoassays (Bio-Rad) based on Luminex technology were used for the  
146 quantification of cytokines, chemokines and growth factors in murine samples,  
147 according to the manufacturer's instruction. A mouse Bio-Plex custom mix was used  
148 to analyze MIP-2, KC, MIP-1 $\alpha$ , IL-6, MCP-1 and TNF- $\alpha$  in murine lung  
149 homogenates. Results were expressed as pg/500ug protein of lung homogenate.

150 The three isoforms of TGF- $\beta$  (TGF- $\beta$ <sub>1</sub>, TGF- $\beta$ <sub>2</sub> and TGF- $\beta$ <sub>3</sub>) were analyzed with Bio-  
151 Plex Pro<sup>™</sup> TGF- $\beta$  3-plex panel in murine BAL fluid and lung homogenates.

152 Data were measured on Bio-Plex 200 System and calculated using Bio-Plex Manager  
153 6.0 and 6.1 software. Levels were expressed as pg/total BALF and pg/500ug protein  
154 of lung homogenate for murine samples.

## SUPPLEMENTARY REFERENCES

- 1 Bragonzi, A. *et al.* Sequence diversity of the mucABD locus in *Pseudomonas aeruginosa* isolates from patients with cystic fibrosis. *Microbiology* **152**, 3261-3269, doi: 10.1099/mic.0.29175-0 (2006).
- 2 Bragonzi, A. *et al.* *Pseudomonas aeruginosa* microevolution during cystic fibrosis lung infection establishes clones with adapted virulence. *Am J Respir Crit Care Med* **180**, 138-145, doi:10.1164/rccm.200812-1943OC (2009).
- 3 Cigana, C. *et al.* *Pseudomonas aeruginosa* exploits lipid A and mucopeptides modification as a strategy to lower innate immunity during cystic fibrosis lung infection. *PLoS One* **4**, e8439, doi:10.1371/journal.pone.0008439 (2009).
- 4 Bianconi, I. *et al.* Positive signature-tagged mutagenesis in *Pseudomonas aeruginosa*: tracking patho-adaptive mutations promoting airways chronic infection. *PLoS Pathog* **7**, e1001270, doi:10.1371/journal.ppat.1001270 (2011).
- 5 Verma, N., Chaudhury, I., Kumar, D. & Das, R. H. Silencing of TNF-alpha receptors coordinately suppresses TNF-alpha expression through NF-kappaB activation blockade in THP-1 macrophage. *FEBS Lett* **583**, 2968-2974, doi:10.1016/j.febslet.2009.08.007 (2009).
- 6 Monticelli, L. A. *et al.* Innate lymphoid cells promote lung-tissue homeostasis after infection with influenza virus. *Nat Immunol* **12**, 1045-1054, doi:10.1031/ni.2131 (2011).
- 7 Cersini, A., Martino MC, Martini I, Rossi G, Bernardini ML. Analysis of virulence and inflammatory potential of *Shigella flexneri* purine biosynthesis mutants. *Infect Immun.* **71**, 7002-7013 (2003).

- 8 Martino, M., Rossi G, Martini I, Tattoli I, Chiavolini D, Phalipon A, Sansonetti PJ, Bernardini ML. Mucosal lymphoid infiltrate dominates colonic pathological changes in murine experimental shigellosis. *J Infect Dis.* **192**, 136-148 (2005).
- 9 Dykstra, M., Levisohn S, Fletcher OJ, Kleven SH. Evaluation of cytopathologic changes induced in chicken tracheal epithelium by *Mycoplasma gallisepticum* in vivo and in vitro. *Am J Vet Res.* **46**, 116-122 (1985).
- 10 Nili, H., Asasi K. Avian influenza outbreak in Iran. *Avian Dis.* **47**, 828–831 (2003).
- 11 Noormohammadi, A., Jones JF, Harrigan KE, Whithear KG. Evaluation of the non-temperature-sensitive field clonal isolates of the *Mycoplasma synoviae* vaccine strain MS-H. *Avian Dis.* **47**, 355-360 (2003).
- 12 McLoughlin, D. *et al.* Pravastatin reduces Marfan aortic dilation. *Circulation* **124**, S168-173, doi:10.1161/CIRCULATIONAHA.110.012187 (2011).
- 13 Bergin, D. A. *et al.* Airway inflammatory markers in individuals with cystic fibrosis and non-cystic fibrosis bronchiectasis. *J Inflamm Res* **6**, 1-11, doi:10.2147/JIR.S40081 (2013).